2 PF Ring

2-1 Operation Summary

When the Tohoku earthquake struck on March 11, 2011, the PF-ring had already been shut down as scheduled in the morning. Fortunately, no personnel were injured, and no fires were reported in the PF facilities in the immediate aftermath of the first series of strong earthquakes. The most serious damage to the accelerators was the collapse of quadrupole magnets in the Linac. Consequently, some beam ducts were fractured, and most of the 600-m Linac was exposed to the air. At the PF-ring, one of the vacuum bellows broke and half of the ring was exposed to the air. Details of the earthquake damage and the results of the magnet level survey were reported in Ref. [1]. Temporary recovery of the beam duct was accomplished quickly, and trial operation started in mid-May. The user time scheduled from May to July was cancelled, and was resumed in October 2011.

The timetable of the PF ring and PF-AR operations in FY2011 is shown in Fig. 1. The operation statistics of the PF ring are summarized in Table 1. The statistics for each fiscal year since the commencement of accelerator operation are shown in Fig. 2. The total operation time and actual user time were 4696.0 h and 2809.2 h, respectively. Before the summer shutdown, machine and beamline studies had to be carried out for recalibration, which was necessary after the earthquake; the operation time necessary for these studies was calculated to be 805.2 h. The failure time for this year was 11.7 h, and the failure percentage is shown in Fig. 3. Even in the latter half of FY2011, from October 2011 to March 2012, frequent aftershocks continued in east Japan. Sometimes the beam was dumped by the quake, and sometimes we stopped the beam operation and made a patrol of the ring tunnel according to KEK's safety rules. The number of failures caused by the earthquakes amounted to four or five in FY2011.

In the trial beam operation from May to July, an abnormal rise in vacuum pressure occurred when the single-bunch high-current beam was stored. The elastomer O-ring and the valve disc changed color due to heating as shown in Fig. 4. The RF shield mechanism became incomplete due to the earthquake and an abnormal higher order mode loss occurred in the gate valve. We removed all gate valves of the same type from the storage ring during the maintenance period in 2011. After removal of these gate valves, the quadrupole-mode longitudinal instability disappeared at a regular stored current of 450 mA; the insufficient RF shield presumably made them high impedance sources. Since we have been able to suppress the longitudinal instability without RF phase modulation, the effective brightness of SR beams has been stably improved, especially from the undulators located at the section that has a finite dispersion function [2].

In the PF-ring, the top-up operation mode was fixed as the normal operation mode. The beam current was usually maintained at 450.0 ± 0.1 mA, which corresponded to a current accuracy of $\pm 1 \times 10^{-4}$ at an injection repetition frequency of 2.0 Hz using a pulsed sextupole magnet. User operation of the hybrid mode was conducted for the first time, with a single-bunch current of 50 mA and a multi-bunch current of 400 mA. In addition, the variably polarized undulator was operated at a switching frequency of 10 Hz. Orbit correction using the feed-forward method allowed us to reduce the orbit fluctuation during the switching process to less than a few micrometers.

REFERENCES

[1] T. Honda, et al., *Proc. IPAC'11* (2011) 2984.
[2] *PF Activity Report 2008,* **26** (2010) 124.

Table 1 Operation statistics for PF ring in FY2011.

	Total
Ring operation time (h)	4696.0
Actual user time (h)	2809.2
Machine & BL study	805.2
Machine adjustment time (h)	1069.9
Failure time (h)	11.7

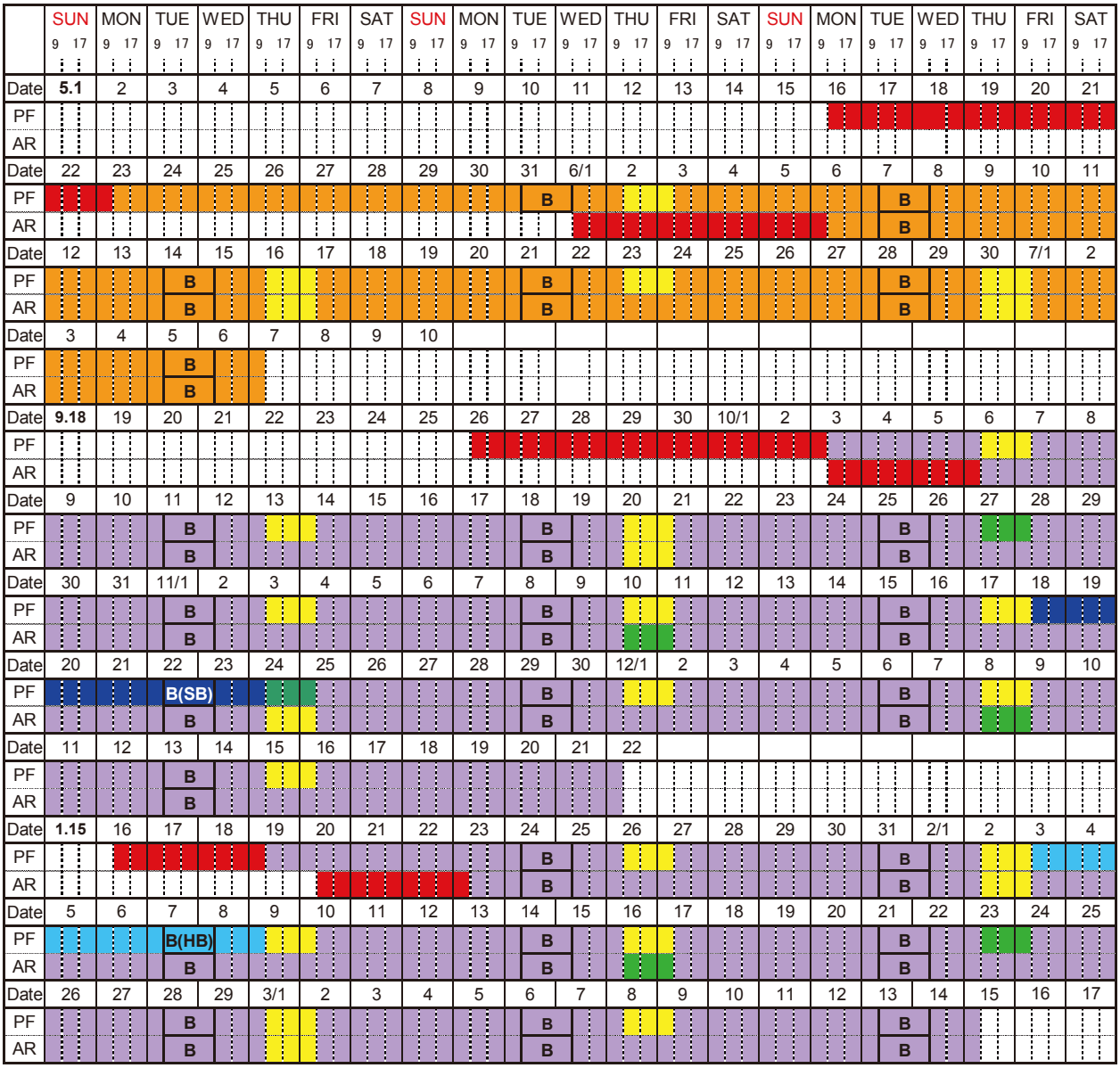

Figure 1
Timetable of PF ring and PF-AR operation in FY2011.

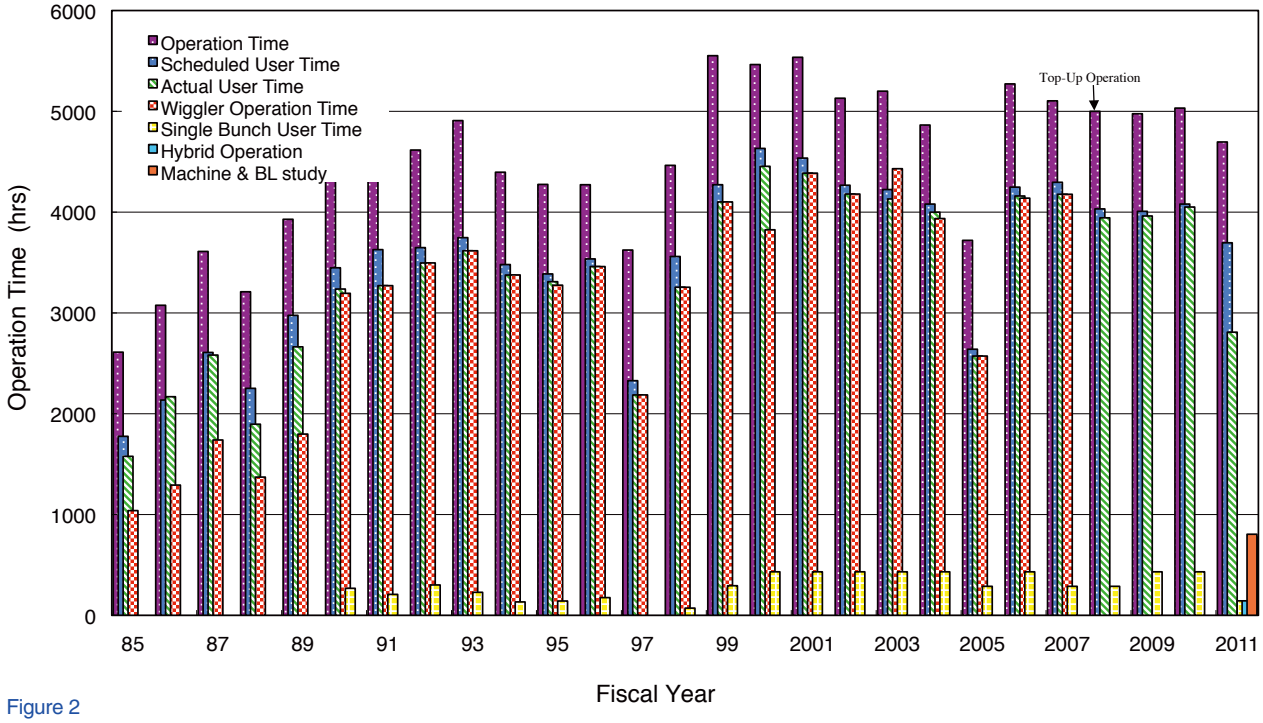

Figure 2
Total operation time, scheduled user time, actual user time, user times of various operation modes, and operation time of the machine and beamline study for PF ring in each fiscal year since commencement of accelerator operation.

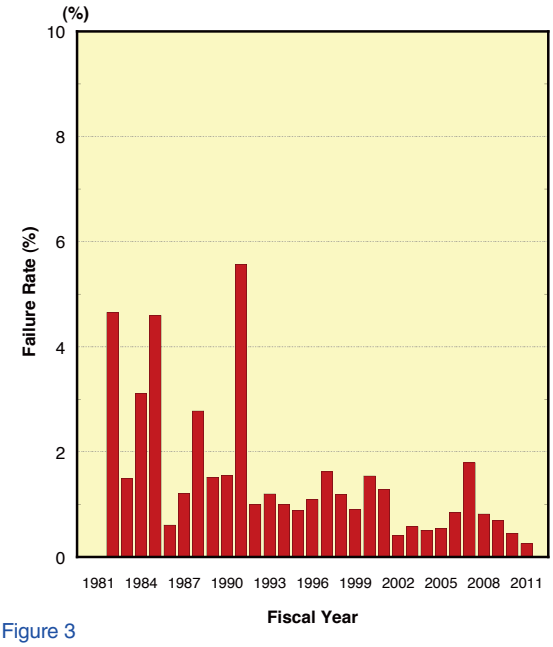

Figure 3
Failure rate for PF ring (percentage of failure time with respect to total operation time).

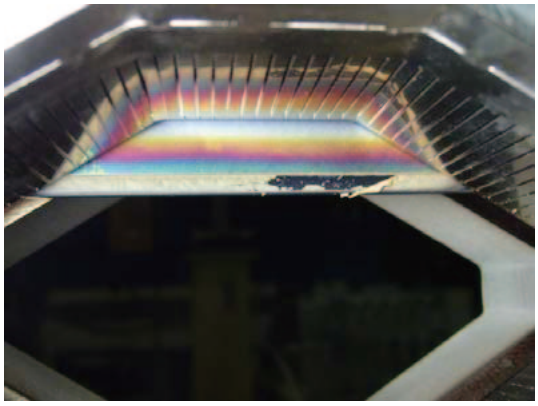

Figure 4
Gate valve damaged by trouble of the RF-shield mechanism.

2-2 ID16 Bump

At the long straight section of 8.9-m length between B15 and B16 at the PF ring, two APPLE-II type undulators were installed with five identical fast bump magnets. The fast local bump achieves fast helicity switching, and is a good method for measuring the photon helicity-dependence of materials like circular and linear dichroism using a lock-in technique. The designed bump frequency is 10 Hz and the required bump angle is 0.3 mrad to separate photons from the two undulators.

In order to achieve user runs with fast local bump, the unwanted beam oscillation around the ring should be suppressed to smaller than 1/10 of the beam size, which is about 30 μm for the horizontal direction and 3 μm for the vertical direction. After system adjustment with feed-forward correction, the 10-Hz beam disturbance was kept small around the ring as shown in Fig. 5. During the test operation on December 8, 2011, all users were asked to measure the effect of the beam disturbance by the 10-Hz fast local bump. The magnitudes of the measured disturbances were most similar to those of the top-up injection for some beamlines, and so permission was given to make the 10-Hz fast local bump during normal user runs. User runs with the 10-Hz bump were conducted during the following periods in FY2011:

09:00, Jan. 19 to 09:00, Jan. 23 (for long-term test)
21:00, Feb. 22 to 09:00, Feb. 23
09:00, Mar. 9 to 08:30, Mar. 12

Operation of the 10-Hz bump was usually started at 08:30 and stopped at 20:30, which are the times of

PF-AR injection and mode change of other insertion devices when small orbit distortions are permitted. The DC orbit distortions shown in Fig. 6 are unavoidable when starting and stopping operation, and future machine studies will examine ways of suppressing these distortions.

During the 10-Hz operation, the users of BL-16 can freely change the parameters ρ and ϕ of ID16-1 and ID16-2, and can freely decide to start and stop operation at two fixed times of the day during fast bump user time. The parameters of the bump kickers and feedforward system are fixed at the beginning of the run and no adjustments are required for several months.

User runs of the 10-Hz fast bump and machine studies for improvements will continue in 2012.

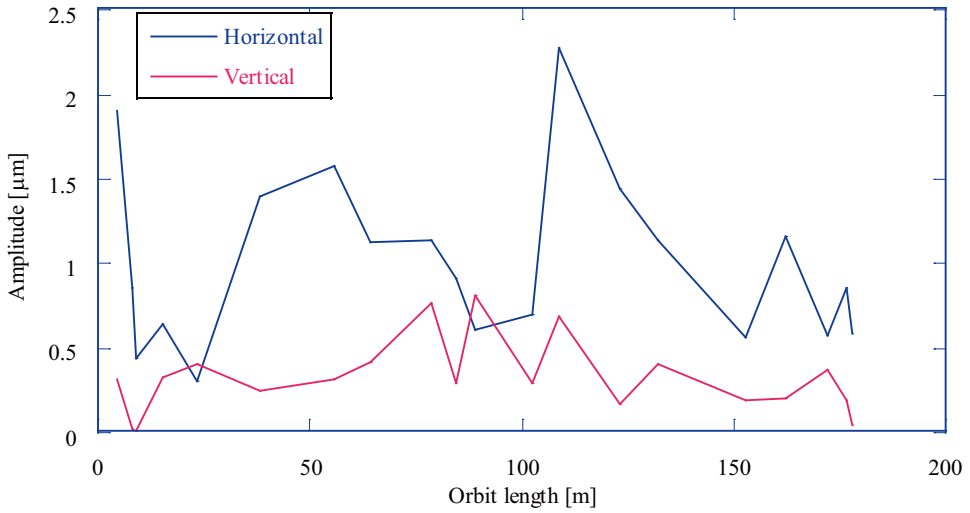

Figure 5
Amplitude of the unwanted 10-Hz beam oscillation around the ring during the 10-Hz fast bump operation.

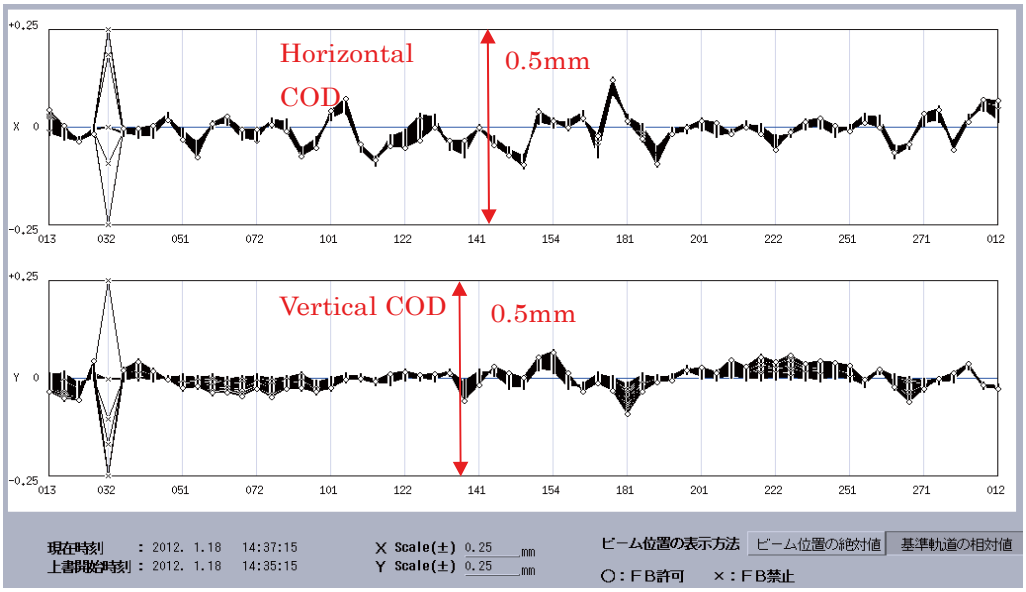

Figure 6
Test measurements of the temporal DC COD change upon starting or stopping the 10-Hz fast bump without vertical fast orbit feedback. For user runs, the vertical changes are much smaller due to the vertical fast orbit feedback correction.

2-3 Introduction of Hybrid Filling Mode

The hybrid filling pattern, which consists of short bunch trains and high-current single bunches, enables us to share the use of limited machine time between multi-bunch and single-bunch users. At the PF-ring, the feasibility of this attractive operation mode has been studied since October 2008 with the development of a free-rotation mechanical light chopper [3, 4]. As the result of resolving technical problems [5] and two joint studies with SR users, user operation with the hybrid filling pattern was achieved in February 2012. This is the first time hybrid operation has been introduced in the PF-ring.

Figure 7 shows the filling pattern in the hybrid mode measured with a beam position monitor. The pattern is composed of 130 low-current bunches (3.1 mA/bunch × 130 = 400 mA) and a high-current single bunch (50 mA/bunch) located on the opposite side of the ring from the bunch train. A total stored current of 450 mA is achieved, the same as usual multi-bunch operation. We succeeded in maintaining the hybrid filling pattern for six days by the flexible top-up injection [6] without any trouble. The coupled-bunch instabilities in the multi-bunch component were completely suppressed by using a bunch-by-bunch feedback system [7]. The single-bunch impurity was kept below 10^{-6} by a gated RF-knockout. Figure 8 compares temperature distributions along the ring between the hybrid and usual single-bunch operations. These distributions are similar to each other with the exception of temperatures around the ceramic duct for the RF-Q magnet and the bellows duct downstream of VW#14. The RF-Q ceramic duct where a relatively large amount of heat generation was observed is scheduled to be removed during the summer maintenance of 2012. A streak image of the hybrid filling pattern is shown in Fig. 9. The RMS bunch lengths of the multi-bunch and single-bunch components were measured to be 37 ps and 56 ps, respectively. The lifetimes of each component were also measured to be around 9 hours and 2 hours, respectively: the lifetime of the single-bunch component is much shorter than that of the multi-bunch component due to the Touschek effect. We will modify the contents of the hybrid operation based on evaluations and requests of users.

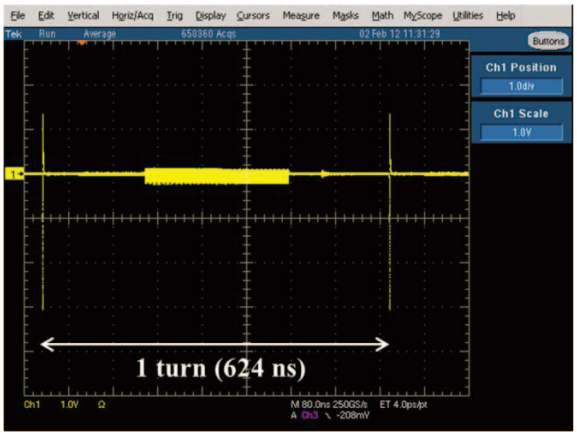

Figure 7
Hybrid filling pattern consisting of 130 low-current bunches (3.1 mA/bunch × 130 = 400 mA) and a high-current single bunch (50 mA/bunch) located on the opposite side of the ring from the bunch train.

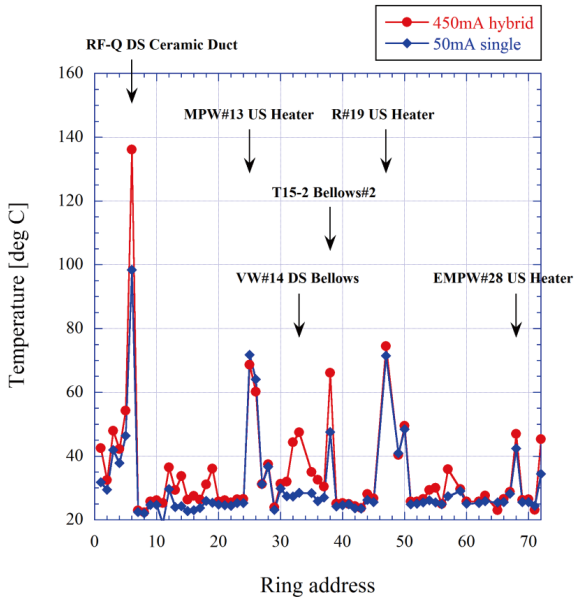

Figure 8
Comparison of temperature distributions along the ring between the hybrid and usual single-bunch operations.

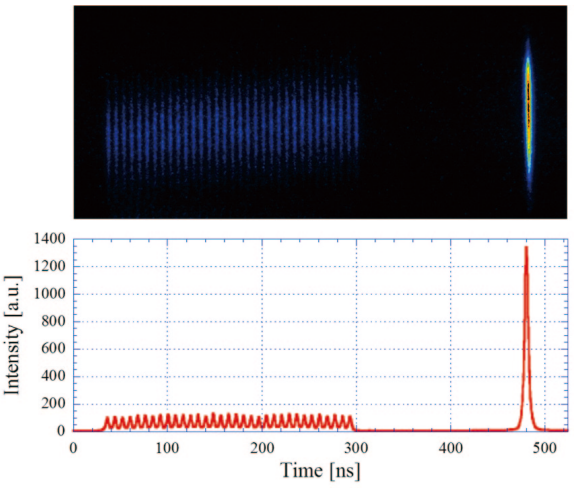

Figure 9
Hybrid filling pattern observed with a streak camera. The upper part shows the two-dimensional streak image, and the lower part shows the relative bunch intensity plotted against time.

REFERENCES

[3] K. Ito, F. Penent, Y. Hikosaka, E. Shigemasa, I. Suzuki, J. Eland and P. Lablanquie, *Rev. Sci. Instrum.*, **80** (2009) 123101.
[4] *Photon Factory Activity Report 2008*, **#26** (2010) A125.
[5] R. Takai, T. Obina, Y. Tanimoto, T. Honda, M. Shimada, Y. Kobayashi and T. Mitsuhashi, *Proc. IPAC'10* (2010) 2564.
[6] *Photon Factory Activity Report 2009*, #**27** (2011) A114.
[7] *Photon Factory Activity Report 2009*, #**27** (2011) A113.

2-4 Development of Optical Fiber Beam Loss Monitor for the Photon Factory

A beam loss monitor using optical fibers has been developed to determine the loss point of the injected beam at the Photon Factory 2.5-GeV electron storage ring. Large-core optical fiber was installed along the vacuum chamber of the storage ring in order to cover the whole storage ring continuously. In total, 10 optical fibers with the length of 30 m are used. Both ends of the fiber are fed out of the radiation shield of the ring, and a photomultiplier tube (PMT) is attached on the upstream side of the fiber. If the electrons are not captured in the storage ring, they will hit the vacuum chamber and produce secondary electrons. Then the electrons that pass through the glass core of the optical fiber produce Cherenkov light. The sensitivity of the PMT (Hamamatsu H10721-110) is sufficiently high to detect the loss at the PF ring, and its short rise-time of about 0.6 ns is fast enough to determine the location of the beam loss point.

Figure 10 shows an example beam loss during injection measured from B12 to the vertical wiggler, VW14. The blue line (CH1) and the red line (CH2) show the beam loss detected at the outer-side and inner-side of the storage ring, respectively. The peak is clearly located at the vacuum chamber with bellows. The distance between components and the corresponding time-difference between pulses does not match in some locations because the optical fiber cannot be laid straight and deviates outside the components. For example, the vertical superconducting wiggler (VW14) has a large body, and so the length of the optical fiber is much longer than the electron orbit length.

In the KEK-PF, two kinds of injection system have been used for routine operation: kicker magnets and a pulsed sextupole magnet (PSM). The fiber loss monitor is useful for analyzing the turn-by-turn difference of the beam loss pattern. Figure 11 shows an example of PMT voltage with the two injection methods. The kicker injection indicates a large loss at the first turn and fourth turn, whereas the PSM injection shows no loss of beam at the first turn, but a large loss at the second turn. Detailed analysis is under way, and the monitor will be used for injection tuning.

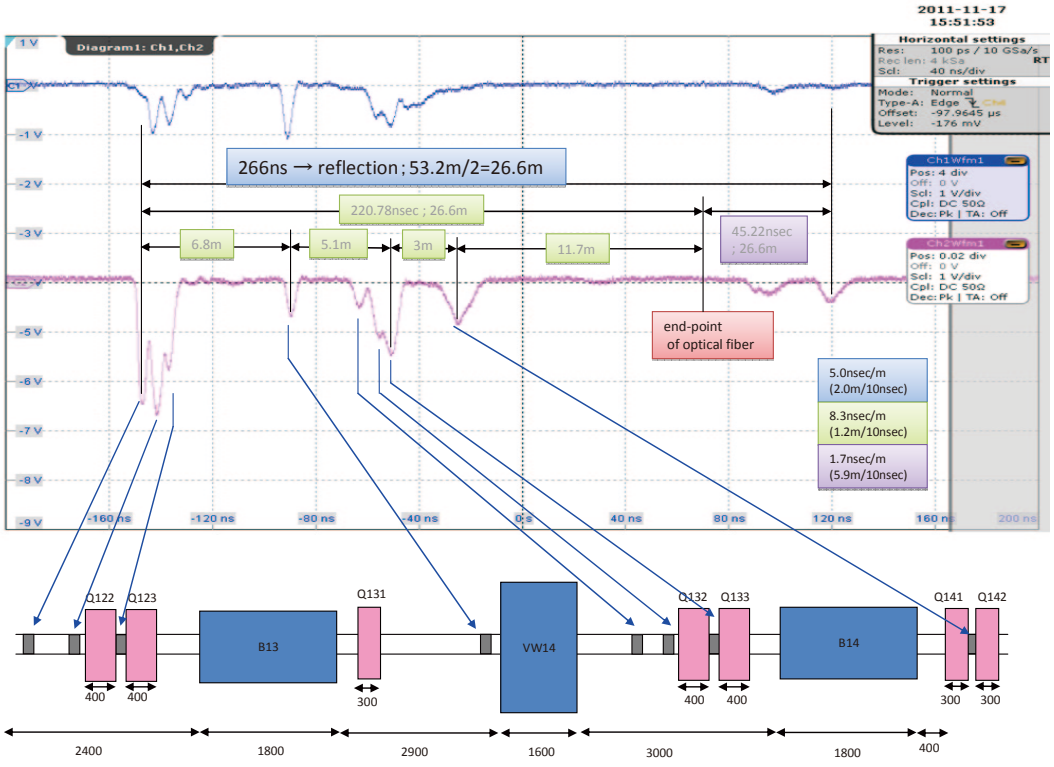

Figure 10
Example of beam loss signal and layout of storage ring components.

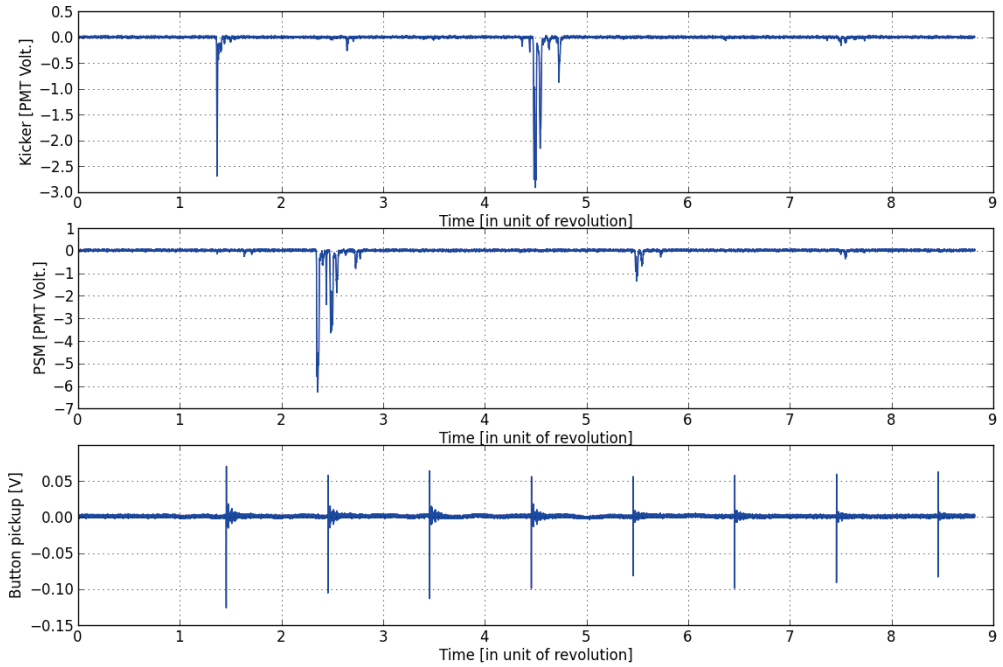

Figure 11
Beam loss signal with two injection methods. Upper and middle figures show the PMT output voltage for kicker injection and PSM injection, respectively. The bottom figure shows the results for a button-type pickup electrode near the loss monitor.

2-5 Project to Renew the Insertion Devices at the PF Ring

2-5-1 A New Short Gap Undulator (SGU#15)

At the PF ring, we constructed three short gap undulators (SGU) at the four short straight sections of 1.4-m length. For the remaining straight section, B14-15, we are planning to construct a new SGU#15 as a light source for both small-angle X-ray scattering experiments and XAFS experiments. SGU#15 will be the fourth SGU, with a period length of 17.6 mm, number of periods of 27 and maximum deflection parameter of 1.61. The photon energy region of SGU#15 is wide, from 2 keV to 15 keV. To cover this entire energy region, the higher harmonics of undulator radiation will be used up to the 9th higher harmonics. Figure 12 shows a calculated spectrum of SGU#15. Construction of SGU#15 will be finished by the end of 2012 and we will install it in the PF ring in the summer of 2013.

2-5-2 Design of the Undulators for the VUV-SX Light Source Renewal Project

As part of the VUV-SX beamline renewal project, we are investigating the design of the new undulators for BL-02, BL-13 and BL-28, which will be called U#02-2, U#13 and U#28, respectively. All these undulators are designed as elliptically polarizing undulators (EPUs) to

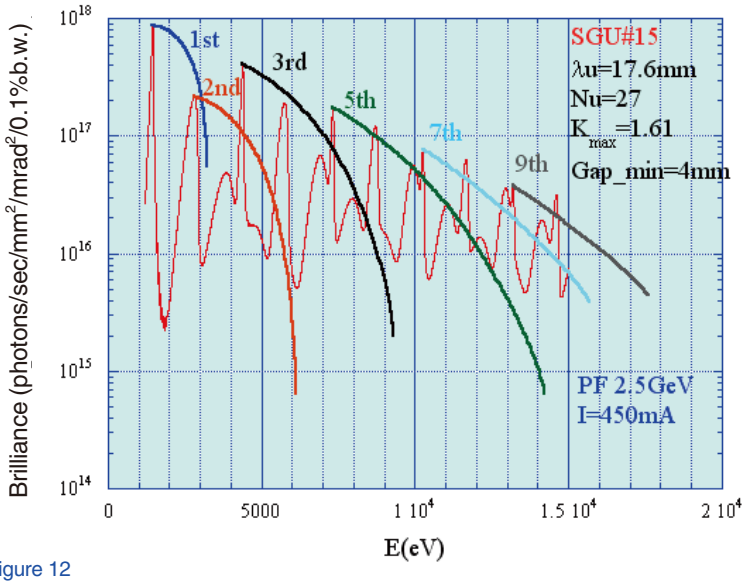

Figure 12
Calculated spectrum of SGU#15.

obtain various polarization states, not only circular (left-handed and right-handed) polarization but also linear (horizontal and vertical) polarization. We renewed the present undulators for BL-13 and BL-28 to utilize the extended straight section effectively. For BL-02, we plan to move the existing undulator (U#02) to the downstream of the B01-B02 straight section, and install a new undulator (U#02-2) tandem at the upstream of U#02. We will use U#02 and U#02-2 exclusively to obtain photons over a wide energy region at the single beamline. The photon energy region of U#02 is from 400 eV to 2 keV and the target energy region of U#02-2 is from 15 eV to 300 eV with the first harmonic radiation of EPU.

Table 2 shows the designed parameters of the new undulators. The period length of both U#02-2 and U#28 is 160 mm, while that of U#13 is under investigation and is around 80 mm. Figure 13 shows typical calculated spectra of U#13 and U#28. Figure 14 compares the spectral properties of U#02 and U#02-2.

We will construct these three undulators by fiscal 2013 and install them in the PF ring step by step during 2014.

Table 2 Basic parameters of the new undulators in the PF ring.

Name	Period length (mm)	Number of periods	Length (m)	Maximum Bx, By (T)	Target photon energy region (eV)	Type of undulator
U#02-2	160	17	2.72	0.33, 0.33	30-300	EPU
U#13	76	47	3.57	0.68, 0.34	50-1500	EPU
U#28	160	22	3.52	0.33, 0.33	30-300	EPU

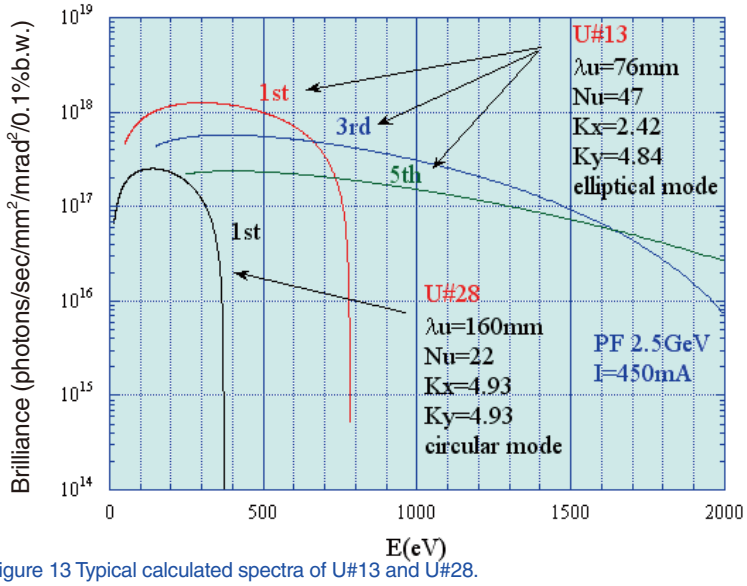

Figure 13 Typical calculated spectra of U#13 and U#28.

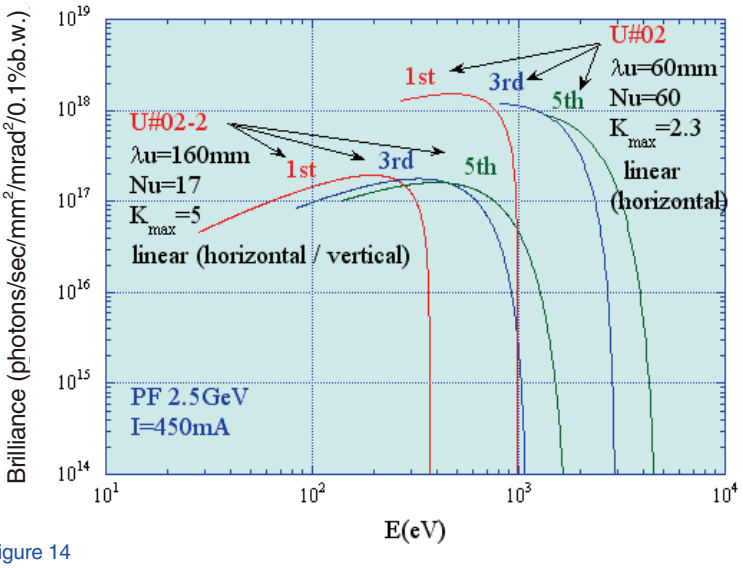

Figure 14
Comparison of photon energy region of U#02 and U#02-2.